Vision Research 58 (2012) 33–44

Contents lists available at SciVerse ScienceDirect

Vision Research

journal homepage: www.elsevier.com/locate/visres

Characteristics of the filled-in surface at the blind spot

Yihwa Baek [a], Oakyoon Cha [a], Sang Chul Chong [a,b,*]

[a] Graduate Program in Cognitive Science, Yonsei University, Seoul, Republic of Korea
[b] The Department of Psychology, Yonsei University, Seoul, Republic of Korea

ARTICLE INFO

Article history:
Received 17 August 2011
Received in revised form 28 January 2012
Available online 28 February 2012

Keywords:
Blind spot
Filling-in
Contour integration
Binocular rivalry
Perceptual waves

ABSTRACT

Our visual system can restore information missing within the portion of the retinal image corresponding to the blind spot where the optic nerve exits the eye. Previous studies of the properties of filled-in surfaces at the blind spot have found similarities and dissimilarities between filled-in and real surfaces and have therefore not provided a consistent view of the characteristics of the filled-in surface. First, we investigated whether filling-in utilizes a contour integration mechanism. Gratings with collinear lines filled in the blind spot more effectively than those both with orthogonal lines and without any line, suggesting that collinear facilitation underlies the filling-in of the blind spot. Second, the dynamics of binocular rivalry was examined by comparing the dominance duration distributions of filled-in and real surfaces. The results indicated that the strength of the filled-in surface was attenuated compared to that of the real surface during rivalry. Lastly, we tested whether travelling waves of dominance in rivalry could occur at the blind spot. The travelling waves could propagate through a hole only at the blind spot, suggesting that the filled-in surface helps perceptual waves to travel across the blind spot. These results suggest that the filled-in surface shares a common mechanism via a horizontal connection but that it has weak strength to suppress the opposite eye during binocular viewing.

1. Introduction

The optic nerve exits the retina at the optic disk, creating a circumscribed area devoid of photoreceptors. Ordinarily we do not perceive this blind spot because it is perceptually filled in by information from the other eye as well as by information from neighboring regions around the blind spot itself (Murakami, 1995; Ramachandran, 1992). This filling-in process is rather remarkable given the relatively large size of the blind spot, which encompasses an ellipse with long and short axes subtending about 6° in width and 8° in height (Armaly, 1969).

Neurophysiological studies have demonstrated that the filled-in information is not merely conceptually noted (Dennett, 1992) but is represented by lateral propagation of neural activity (Komatsu, Kinoshita, & Murakami, 2002; Matsumoto & Komatsu, 2005; Pessoa, Thompson, & Noë, 1998). Due to the active propagation of neural activity from the regions surrounding the blind spot, cortical neurons that have receptive fields corresponding to the blind spot can respond to stimulation imaged within the blind spot region. The consequences of the blind spot, in other words, are minimized by neuronal filling-in (Awater et al., 2005; Tripathy et al., 1995).

Previous studies of the characteristics of surface completion within stimuli outside of the blind spot have concluded that filled-in surfaces are comparable to what one would expect to see based on the stimulus actually presented (Komatsu, 2006; Lleras & Moore, 2006; Shimojo, Kamitani, & Nishida, 2001). However, whether or not this is true in the case of the blind spot remains debatable. Murakami (1995) showed that adaptation to visual motion within the blind spot generated a motion aftereffect (MAE) at the corresponding location of the other eye, albeit a weaker MAE than that experienced when adapting and test stimuli were both presented to the same eye. In addition, He and Davis (2001) showed that when a stimulus presented around the blind spot induced filling-in, the visibility of a stimulus in the opposite eye was reduced as compared to when the blind spot was not filled in. Those authors suggested that the filled-in surface at the blind spot contributes to binocular rivalry. However, other studies imply differences between the filled-in surface at the blind spot and a corresponding, real surface. Cumming and Friend (1980) found that filled-in stripes at the blind spot were not strong enough to produce tilt aftereffects. Maertens and Pollmann (2007) also demonstrated that the performance of an illusory curvature discrimination task at the blind spot was worse than at a corresponding eccentricity outside the blind spot.

In the present study, the characteristics of the filled-in surface at the blind spot are investigated further by comparing a filled-in surface to a real surface using several different phenomena in an

* Corresponding author at: The Department of Psychology, Yonsei University, Seoul, Republic of Korea. Fax: +82 2 2123 3240.
E-mail address: scchong@yonsei.ac.kr (S.C. Chong).

0042-6989/$ - see front matter © 2012 Elsevier Ltd. All rights reserved.
doi:10.1016/j.visres.2012.01.020

effort to shed light on how a filled-in surface is represented within different visual contexts. Experiment 1 tested whether the collinearity of stimuli facilitates filling-in. Experiment 2 examined how the filled-in surface at the blind spot contributes to binocular rivalry. Lastly, Experiment 3 investigated whether percept changes can propagate through the blind spot with the aid of the filled-in surface during rivalry. Sinusoidal gratings rectangular in shape were used as stimuli in all three experiments, but different experimental paradigms were used across the three experiments.

2. Experiment 1: effects of collinearity and orientation differences on filling-in at the blind spot

To fill in the blind spot, stimuli need to be presented to both sides of the blind spot. A minimal stimulus length (0.33–1.5°) is required to fill in the gap (Abadi, Jeffery, & Murphy, 2011; Kawabata, 1983; Spillmann et al., 2006). According to Field, Hayes, and Hess (1993), elements are more easily integrated into a contour if they have small orientation differences. Moreover, when the orientation difference is held constant, elements collinearly aligned to the path of a contour are more likely to be integrated into the contour than are orthogonally aligned elements. This contour integration mechanism is critical for figure-ground segregation (Geisler et al., 2001; Grossberg & Mingolla, 1985). Experiment 1 examined whether the results found in contour integration can be applied to the blind spot by measuring the minimal stimulus length needed to promote filling within the blind spot. Specifically, we investigated whether the minimal stimulus length for filling-in differed depending on collinearity and orientation differences.

2.1. Material and methods

2.1.1. Observers

Six graduate students of Yonsei University including the first two authors participated in this study. All had normal or corrected-to-normal vision. Every aspect of this study was carried out in accordance with the Institutional Review Committee of Yonsei University. Written, informed consent was obtained from each observer (except the authors) prior to participation.

2.1.2. Apparatus

Stimuli were created using the Psychophysics Toolbox of MATLAB (Brainard, 1997; Pelli, 1997). To present different stimuli to the two eyes separately, two monitors (Samsung SyncMaster T220; refresh rate, 60 Hz; resolution, 1680 × 1050) and a mirror stereoscope were used. Owing to the stereoscope, observers could maintain both eyes open, even for monocular presentation of stimuli. Observers steadied their heads using a chin-and-forehead rest, and the viewing distance was 80 cm. At this distance, one pixel subtended approximately 0.024°.

2.1.3. Blind spot measurement

To measure the size and location of the blind spot for each individual, we employed two tasks, one of which located the center (Fig. 1A and B) of the blind spot and the other which estimated the circumference of the blind spot (Fig. 1C and D). A cross surrounded by a circle of dashes was used for fixation. The fixation was placed vertically in the middle of the video screen (about 12.6° from the top) and 6° away from either the left or right edge of the display depending on the blind spot eye (dominant eye because the blind spot was always measured in the dominant eye). The fixation cross was seen by both eyes, but the dashes were shown interocularly to facilitate binocular alignment. Neighboring dashes were shown to different eyes. First, a small, white dot 0.2° in diameter was moved along a horizontal path extending from the fixation cross at a speed of 1.2 deg/s (Fig. 1B①). The observer pressed the 'space' bar whenever the moving dot first disappeared (i.e., entered the blind spot) and then again when the dot first reappeared (i.e., emerged from the far side the blind spot). After the key press, the dot reversed its direction and the same procedure was followed for the motion toward the fixation mark. This cyclic procedure continued until two consecutive measurements at the same

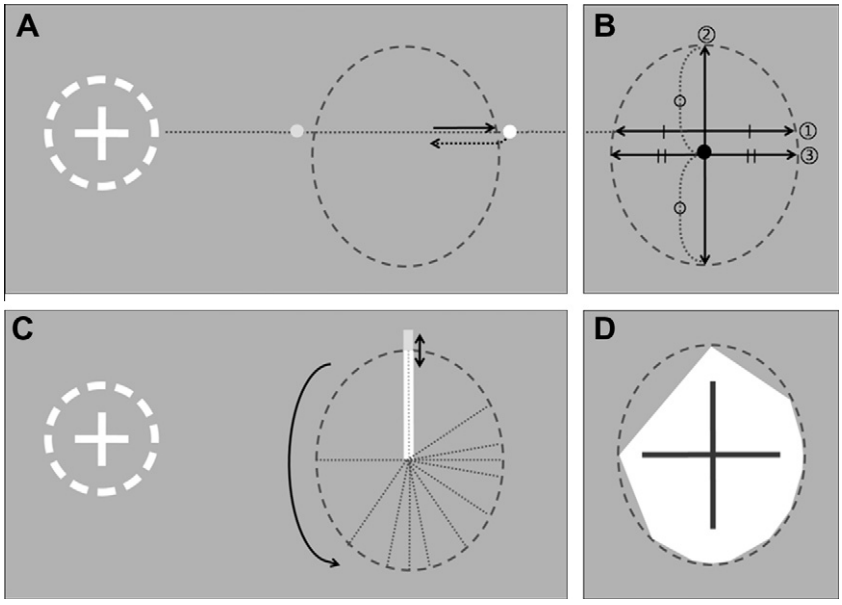

Fig. 1. The blind spot measurement procedure of the center (A and B) and end points at the twelve test locations (C and D). In this figure, the right eye blind spot measurement is described. For the left eye blind spot, everything was mirrored. (A): Observers pressed the space bar whenever a white dot first disappeared and re-appeared again outside the blind spot, after which the dot reversed its direction. (B): The process described in (A) was repeated in the order of (①, ②, and ③) and the center of the blind spot was determined (filled circle). (C) Twelve test locations were measured in turn starting from 0° (indicated by the white radial line) and proceeding counterclockwise (right eye) or clockwise (left eye). Observers adjusted the length of the radial line to the length at which the line just became visible or invisible. (D) By connecting the twelve measured points, the blind spot indicator was created. A red cross (a large gray cross in the blind spot) was imposed on the blind spot indicator to ensure stable fixation. Note that only the red cross was present during the experiment.

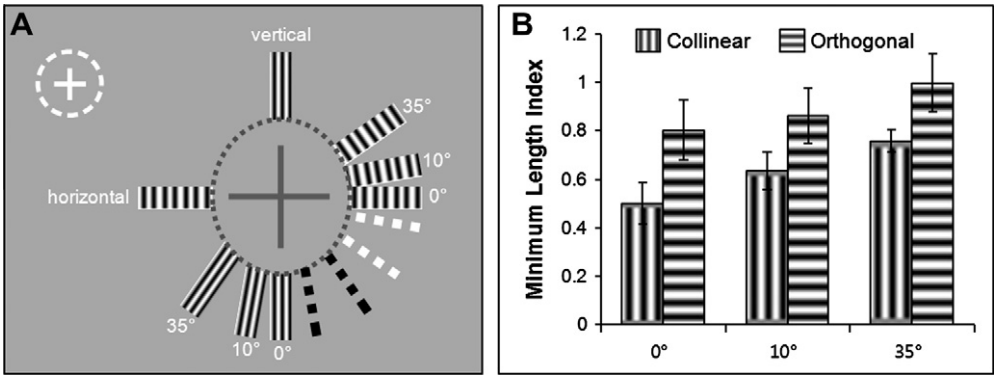

Fig. 2. The stimuli and results of Experiment 1. (A) A schematic diagram of the test locations and sinusoidal gratings of rectangular shape is shown to help clarify the results (not drawn to scale). Collinear test gratings are shown in the vertical condition and orthogonal gratings are shown in the horizontal condition. There were five test locations for each horizontal and vertical condition. However, only three of them are shown here for each condition, collapsing the same orientation differences (e.g., ±10°). The black (vertical condition) and the white (horizontal conditions) dotted bars indicate the original test locations before the collapse. (B): The results of Experiment 1. Error bars indicate the s.e.m.

location differed by less than 0.3°. The criterion of 0.3° had to be satisfied for both sides of the blind spot. Once two end points of the blind spot on the horizontal extension of the fixation cross were measured successfully, the dot was moved vertically along a line which went through the center between the two points denoting the horizontal margins of the blind spot (Fig. 1B②). The vertical extent of the blind spot was obtained using the same method and the same criterion as that used for assessing the blind spot's horizontal extent. After finding the vertical center, the dot was moved horizontally along a line passing through the center of the vertical meridian (Fig. 1B③) and the horizontal meridian of the blind spot was measured. The intersection between the horizontal and vertical meridians defined the center of the blind spot.

To define the circumference of the blind spot, we used a procedure whereby a thin line (0.2° width) slowly increased in length starting at the center of the blind spot (as defined above) by pressing a key until the observer first saw it emerge from the blind spot and by pressing another key which caused the line's length to begin shortening until the observer released the key to denote its disappearance. This cycle continued until the observer's key presses reliably located this point of visible/invisible transition. This procedure was repeated for 12 different radial paths from the center of the blind spot (Fig. 1C). Ten of the twelve end points were test locations and two were used as reference locations. This procedure started with the vertical upward bar (0°) which was the reference for the vertical conditions. The next step was a horizontal bar toward fixation (90°) which was the reference of the horizontal conditions. The remaining radial lines grew out to spots where the minimal stimulus lengths were to be measured (145°, 170°, 180°, 190°, 215°, 235°, 260°, 270°, 280°, and 305°). Finally, the end points of those lines were connected by straight lines to form a polygon shape defining the borders of the blind spot (Fig. 1D). The polygon shape (blind spot indicator) was painted white, 0.6° inside the borders of the blind spot, and its luminance was 100.30 cd/m^2. Inside the polygon shape, a red cross was placed to ensure stable fixation (Araragi & Nakamizo, 2008). The two arms of the red cross were the same in length and the length was the shortest radius of the blind spot. Their width was 0.1°. The blind spot indicator was used only once in the beginning of an experiment to confirm the accuracy of the boundary, but the red cross was always presented throughout the experiment. The average distance from the fixation point to the center of the blind spot for six observers was 14.72°. The average height and width of the blind spot was 6.64° and 5.83°, respectively, values similar to those reported by Armaly (1969).

2.1.4. Main experiment

2.1.4.1. Stimuli. The experimental display consisted of the fixation point and the test gratings (Fig. 2A). Test stimuli were presented only to the blind spot eye (Fig. 2A). Sinusoidal gratings of rectangular shape were used as test stimuli to measure the minimal stimulus length for filling-in of the blind spot (Araragi & Nakamizo, 2008; Tripathy et al., 1995). The width of the gratings was defined as the shortest radius of the individually measured blind spot for each observer, and it ranged from 2° to 2.76°. The length of a reference grating was 3.6° from the edge of the blind spot. The grating's spatial frequency was 2.5 cycles per width of a grating. The background luminance was 52.02 cd/m^2. The Michelson contrast of the test grating was 99.77%.

2.1.4.2. Design. There were three within-subject variables. The first was the type of grating which filled in the rectangles: this was either collinear or orthogonal to the orientation of the rectangles (Fig. 2A). The second variable was the orientation difference between the reference and test gratings: this difference was 0°, ±10°, or ±35°. The maximum orientation difference was set to 35° according to Kawabata (1982). In that study, a dotted line did not fill in the blind spot above an orientation difference of 35°. The third variable was the location of the reference grating: it was either 0° or 90°. Accordingly, the overall configuration of the experimental stimulus was vertical or horizontal (Fig. 2A). We used both vertical and horizontal displays because there is an anisotropy in the minimal stimulus length when filling in the blind spot with vertical vs. horizontal lines (Araragi & Nakamizo, 2008). Also, it would be unclear as to whether the consequent effect was due to the orientation or collinearity of the grating if only one of the conditions were used, either the horizontal or the vertical condition, as the collinear grating of the horizontal condition was horizontal and the collinear grating of the vertical condition was vertical. All of the conditions were randomized in a block, and there were eight blocks, resulting in a total of 160 trials (2 gratings × 5 orientation differences × 2 types of display × 8 blocks = 160 trials). There were two types of blocks depending on the initial length of the test gratings. It was 0° in one block and 4° in the other block. Each block was repeated twice and the order of the series was counterbalanced across observers.

2.1.4.3. Procedure. At the beginning of the main experiment, observers were shown two examples of the filled-in configuration so that they could judge whether the subsequent experimental displays were perceived as filled in based on these examples. For the examples, a 10° collinear test grating and a 35° orthogonal test

grating of the vertical condition were used. These examples consisted of combinations of collinear or orthogonal gratings with two different orientation differences. Also, the distance of the stimulus segments from the fovea within a display was similar in the vertical condition, leading to a more confident filling-in experience. Each test grating was 6° in length to facilitate filling-in across the blind spot. After confirming that the two gratings were perceived as connected, the observers proceeded to the main experiment.

The beginning of each trial involved presentation of the fixation cross, a frame of dashed bars, the blind spot indicator, and the red cross. Observers checked fixation to insure that the dashed bars were aligned to form a circle around the fixation cross. They also made sure that the blind spot indicator was invisible.

While maintaining fixation, observers pressed the 'space' bar and the blind spot indicator disappeared, leaving only the red cross. A reference and a test grating were then presented at the previously measured edges of the blind spot. We used the method of adjustment to measure the minimal stimulus length. Observers adjusted the length of the test grating until they perceived a filled-in grating. When they pressed either the '1' or the '2' key, the length of the test grating either decreased or increased by 0.02°, respectively. When the reference and the test grating were perceived as a connected grating, not as two discrete gratings, the observers pressed the 'space' bar to move onto the next trial. There was no time limit, and observers modified the length of the test grating back and forth to find the minimal stimulus length that just filled in the blind spot. The length of the test grating at which the reference and the test grating were perceived as one was taken as an indicator of how easy filling-in occurred across the gap: shorter test gratings indicated that the filling-in was easier. Before moving onto the next trial, the observers were instructed to check their fixation. If they saw the any section of the red cross protruding from the blind spot, they were encouraged to check their fixation again.

2.2. Results and discussion

The sizes and the shapes of the blind spot varied among observers, and the criterion for complete filling-in could also differ across observers. Thus, the minimal stimulus length was normalized before the analysis. The normalized minimal stimulus length (Minimal Length Index: MLI) was defined in the following way:

$$\mathrm{MLI} = \text{measured length}/\mathrm{R}$$

Here, R indicates the individually measured radius of the blind spot. We used a horizontal radius when we normalized the measured lengths in the horizontal displays and used a vertical radius for those in the vertical displays. We used a different radius due to the known anisotropy in the shape of the blind spot (Armaly, 1969).

The results of the main experiment are shown in Fig. 2B. In the following analyses, we report Huynh–Feldt corrected p values. A repeated-measures ANOVA showed the main effect of collinearity. Collinear gratings (Mean MLI: 0.66) filled in the blind spot with a shorter minimal stimulus length than the orthogonal gratings (Mean MLI: 0.91; $F(1,5) = 17.59$, $p < .01$). The main effect of the orientation difference was also significant ($F(2,10) = 10.11$, $p < .05$), indicating that a greater orientation difference required a larger MLI. The MLIs of the vertical and horizontal displays were not significantly different ($F(1,5) = 0.80$, $p = .41$) and the data were collapsed for the subsequent analyses. There was no significant interaction between the variables.

Paired-sample t-tests were performed to determine which specific conditions showed statistically significant differences. The MLI of the collinear condition was significantly different from the orthogonal condition in all orientation difference conditions (0°: $t(5) = 5.70$, $p < .01$; 10°: $t(5) = 4.64$, $p < .01$; 35°: $t(5) = 2.66$, $p < .05$). The MLIs of the orientation differences differed from each other only when the grating was collinear (0–10°: $t(5) = 3.80$, $p < .05$; 0–35°: $t(5) = 4.78$, $p < .01$; 10–35°: $t(5) = 3.49$, $p < .05$). This result was not significant or marginally different when the grating was orthogonal (0–10°: $t(5) = 1.54$, $p = .19$; 0–35°: $t(5) = 2.11$, $p = .09$; 10–35°: $t(5) = 2.44$, $p = .06$).

Additionally, we tested whether collinear gratings facilitated the filling-in process or orthogonal gratings hindered it to produce the main effect of collinearity. We tested an additional condition in which we presented a rectangle without gratings (solid condition). Repeated-measures ANOVA showed that the collinear condition had significantly shorter MLIs than the solid condition ($F(1,3) = 19.01$, $p < .05$). However, the MLIs of the orthogonal and solid conditions were not significantly different ($F(1,3) = 0.07$, $p = .81$). These results indicated that the difference observed between the collinear and orthogonal conditions was due to collinear facilitation.

In summary, we found that the effects of collinearity and the orientation difference apply to the blind spot region. The collinear grating filled-in the blind spot more effectively than did the orthogonal grating, consistent with the stronger contour integration of collinear Gabor-patches (Field, Hayes, & Hess, 1993). Also, two separately presented gratings appeared to be connected more easily when their orientation difference was smaller. These results suggest that the filling-in process at the blind spot follows rules that are similar to those in both the contour integration of Gabor patches (Field, Hayes, & Hess, 1993) and in amodal completion (Kellman & Shipley, 1991).

3. Experiment 2: temporal dynamics of filled-in and real surfaces during binocular rivalry

The results of Experiment 1 do not involve a direct comparison of completion within the blind spot and completion within a region outside the blind spot. Thus we are unable to say to what extent the filled-in surface at the blind spot differed from the quality of filling-in that would be observed outside the blind spot. It is possible, however, to compare the blind spot and a normal region using binocular rivalry when both regions can be tested with the same stimulus.

Several studies have demonstrated that the filled-in surface represented at the blind spot can compete with a real surface (He & Davis, 2001; Shin, Jung, & Chong, 2007; Tong & Engel, 2001). For example, He and Davis (2001) found that a filled-in radial grating presented at the blind spot competed with a circular grating in the opposite eye. However, it has yet to be investigated whether the strength of the filled-in surface at the blind spot is different from that of a real surface.

Tong and Engel (2001) found that the mean dominance duration of a filled-in surface was shorter than that of the real surface during rivalry, in which the filled-in surface at the blind spot competed with the real surface of the opposite eye. Shorter dominance durations associated with the filled-in surface at the blind spot implied that the strength of the filled-in surface was weaker relative to the opposite eye stimulus. However, a comparison between eyes is not appropriate because eye dominance is an important factor in determining rivalry phase durations (Collins & Blackwell, 1974). Instead, to study the effect of filling-in on binocular rivalry, it is necessary to compare dominance durations on a filled-in surface and on a real surface both viewed by the same eye. In the present experiment, we tested whether there were dominance differences between a filled-in and a real surface in an effort to understand the mechanism of the dominance duration difference found by Tong and Engel (2001).

3.1. Materials and methods

3.1.1. Observers

Four observers, including the authors, participated in this experiment. All had normal or corrected-to-normal vision.

3.1.2. Apparatus and stimuli

This experiment used the same settings and software as those used in Experiment 1. The blind spot was always measured in the dominant eye; we will refer to the non-dominant eye as the opposite eye. The fixation cross appeared 8.4° from the top and 7.2° from the left or the right edge of the display depending on the blind spot eye. Examples of the stimuli used in this step are shown in Fig. 3. The rival stimuli were two, orthogonally oriented sinusoidal gratings of rectangular shape with a spatial frequency of 3.5 cpd; the contours of the two rival gratings were oriented 45° clockwise and counterclockwise from vertical. The color of one grating was red and the other green, to help observers distinguish which one of these eccentrically viewed rival stimuli was dominant at any given moment. The Michelson contrasts of the red and the green gratings were 21.07% and 69.49%, respectively. This contrast difference was necessary to equate the brightness of the red and green colors. The length of the stimuli from each side of the blind spot was 2.5°; thus, the total length of the stimuli was the sum of 5° and the horizontal length of the blind spot. The total length of a grating was identical in the non-blind-spot condition. The width of all gratings was 2°. In pilot studies, dominance durations of the blind spot eye were too brief for stable reports of perceptual state. Therefore, we had to reduce the strength of the grating presented in the opposite eye. The size of the grating presented to this eye was reduced by removing the area of 2.5 × 0.5° from every corner of the grating (Fig. 3, opposite eye). Note that although the strengths of the stimuli for the two eyes differed, the strength of stimulus within each eye remained constant because we used the same stimuli within each eye. Because we compared the conditions within each eye, the difference in the strengths in our stimuli across eyes was not critical. To facilitate binocular alignment, rectangular frames with a 0.24° thick line surrounded the gratings. The distance between the frame and the grating was 2°. The area for tracking percept changes due to rivalry (tracking region, Fig. 3 opposite eye) was indicated by four small dots (diameter of each dot was 0.36°). Observers tracked changes in dominance between the rival gratings only within this region to reduce the difficulty of tracking in the periphery. Each dot was 0.8° horizontally and 1.5° vertically away from the center of the blind spot. These dots were always presented to the opposite eye and were thus always visible.

3.1.3. Design

There were three within-subject variables. The first independent variable was the rivalry location: this was at the blind spot of the dominant eye or at the same eccentricity outside the blind spot in the same eye. In the blind spot condition, the stimuli were horizontally presented to both sides of the blind spot. For the same eccentricity condition, the stimuli were presented 3° below the blind spot and at the same eccentricity. The other two variables were the orientation of the gratings (clockwise or counterclockwise) and the color (red or green) of the gratings. Each condition was tested in a 90-s trial, resulting in a total of 8 trials (2 testing locations × 2 grating tilts × 2 colors = 8 trials). The blind spot condition and the same eccentricity condition alternated, and the other variables were randomized across trials. The trials were interleaved with a resting period of 2 min.

3.1.4. Procedure

Before the main experiment, the blind spot of each observer's dominant eye was measured using the same procedure described in Experiment 1, except that 8 points were used instead of 12 to draw a blind spot indicator. The boundary of the blind spot was determined for the horizontal and vertical meridians, and the other 4 points were measured at ± 30° orientations from the orientation of the gratings.

At the beginning of each trial, the fixation cross and the blind spot indicator appeared so that observers could verify their fixation. The blind spot indicator disappeared after the fixation check. Then, rival stimuli were presented to each eye and the observers reported the dominant color percept inside the four dots for 90 s by pressing the '1' key for 45° clockwise and the '2' key for 45°

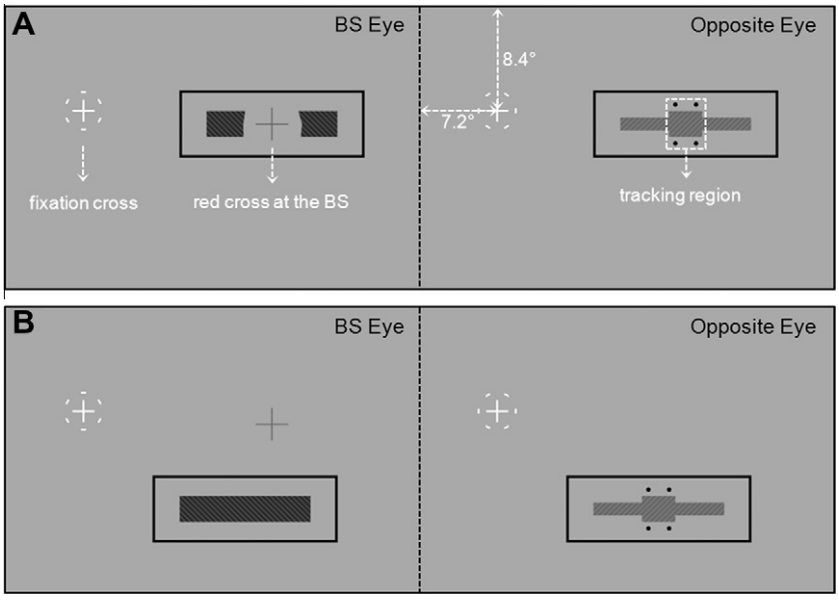

Fig. 3. The stimuli of Experiment 2. (A) The blind spot condition. (B) The same eccentricity condition. In both conditions, the colors (red or green) and grating tilts (clockwise or counterclockwise) of the sinusoidal gratings of rectangular shape differed across eyes. Different shades in the gratings indicate different colors. The color of a gray cross was red, and it was presented in the center of the blind spot to ensure stable fixation.

counterclockwise. Both keys were pressed or released together for a mixed percept.

3.2. Results and discussion

The pattern of average mean phase durations and relative predominance in Fig. 4 suggests that the observers experienced rivalry alternations in both the blind spot condition and the same eccentricity condition. Average mean phase durations of all observers in the blind spot condition (Fig. 4A, light gray) were 3735 ms (s.e.m.: 818 ms) for the blind spot eye, 2023 ms (s.e.m.: 343 ms) for the opposite eye, and 211 ms (s.e.m.: 129 ms) for the mixed percepts. Average mean phase durations in the same eccentricity condition (Fig. 4A, dark gray) were 5884 ms (s.e.m.: 1447 ms) for the blind spot eye, 4240 ms (s.e.m.: 1186 ms) for the opposite eye, and 231 ms (s.e.m.: 120 ms) for the mixed percepts. Fig. 4B shows relative predominance, defined as the percentage of total viewing time that the observers reported perceiving the blind-spot grating only, the opposite-eye grating only or the mixed percepts between the two gratings (Tong & Engel, 2001). Average relative predominance values of all observers in the blind spot condition (Fig. 4B, light gray) were 57.11% (s.e.m.: 2.33%) for the blind spot eye, 38.52% (s.e.m.: 3.65%) for the opposite eye, and 4.37% (s.e.m.: 1.76%) for the mixed percepts. Average relative predominance in the same eccentricity condition (Fig. 4B, dark gray) were 61.38% (s.e.m.: 3.54%) for the blind spot eye, 32.54% (s.e.m.: 4.37%) for the opposite eye, and 6.09% (s.e.m.: 2.59%) for the mixed percepts. The mixed percepts were excluded from further analysis because there were only small portions of mixed percepts during rivalry. In addition, paired-sample t-tests on mixed percepts between conditions were not significant for the mean phase duration ($t(3) = .72$, $p = .53$) or for the relative predominance ($t(3) = 1.66$, $p = .20$).

A repeated-measures ANOVA of the mean phase durations (Fig. 4A) did not show any significant main effect for eye ($F(1,3) = 9.85$, $p = .05$) or condition ($F(1,3) = 7.16$, $p = .08$). In addition, there was no significant interaction between the eye and the condition ($F(1,3) = .15$, $p = .72$). This result may appear to be inconsistent with Tong and Engel (2001) in that it did not show any mean phase duration difference across eyes. However, it should be noted that we reduced the strength of the stimulus presented to the opposite eye by cutting four corners. Cutting the corners not only reduced the strength of the stimulus but also changed the global shape that may influence the mean phase durations (Alais & Blake, 1999). Also, the blind spot eye was always the dominant eye of each observer. A repeated-measures ANOVA of the relative predominance (Fig. 4B) showed a significant main effect of the eye ($F(1,3) = 12.95$, $p < .05$). The main effect of the condition was not significant ($F(1,3) = 2.91$, $p = .19$).

Before further analysis, the data were normalized using the individual baseline mean phase duration (π) of each eye for a comparison across conditions. This normalization process was also done because alternation rates between binocular images varies considerably among individuals (Aafjes, Hueting, & Visser, 1966), making it impractical simply to average dominance values across observers. The baseline mean phase duration was derived from the average dominance duration for the same eccentricity condition. The average baseline mean phase duration of the blind spot eye (mean: 3735 ms; s.e.m.: 818 ms) was marginally longer than that of the opposite eye (mean: 2023 ms; s.e.m.: 343 ms), $t(3) = 3.19$, $p = .05$.

Dominance durations measured for bistable stimuli such as an ambiguous figure or binocular rivalry generally conform to a gamma distribution (Blake, Fox, & McIntyre, 1971; Brascamp et al., 2005; Fox & Herrmann, 1967; Levelt, 1967; Logothetis, 1998). Thus, we fitted a gamma functions to the normalized data (Fig. 5) and carried out the Kolmogorov–Smirnov test (K–S test) to evaluate whether the duration distributions of the two conditions were from the same continuous distribution. The individual two-sample K–S tests for the opposite eye between the dominance duration of the blind spot and the same eccentricity conditions were significant for all observers (all p's $< .05$; mean Kolmogorov–Smirnov $Z = 1.77$). Meanwhile, the K–S test results for the blind spot eye between the dominance durations of the two conditions were not significant ($p = .62$, .50, and .20 each; mean Kolmogorov–Smirnov $Z = 0.88$) except for one observer, S3 ($p < .01$; Kolmogorov–Smirnov $Z = 1.64$), whose percept alternated faster than the percepts for the rest of the observers. His mean phase duration of the dominant eye (i.e., the blind spot eye, 1.4 s) was not particularly longer than that of the opposite eye ($\pi = 1.2$ s) as compared to the other observers. As illustrated in Fig. 5B, the shapes of the dominance duration distributions of the opposite eye involved fewer short-duration events and more long-duration events in the blind spot condition than in the same eccentricity condition.

We found that filling-in of the blind spot influenced the distribution of dominance durations in the opposite eye more than that of the blind spot eye. This is consistent with Levelt's second proposition (Levelt, 1968; Mueller & Blake, 1989), which holds that changing the stimulus strength of an eye affects the suppression

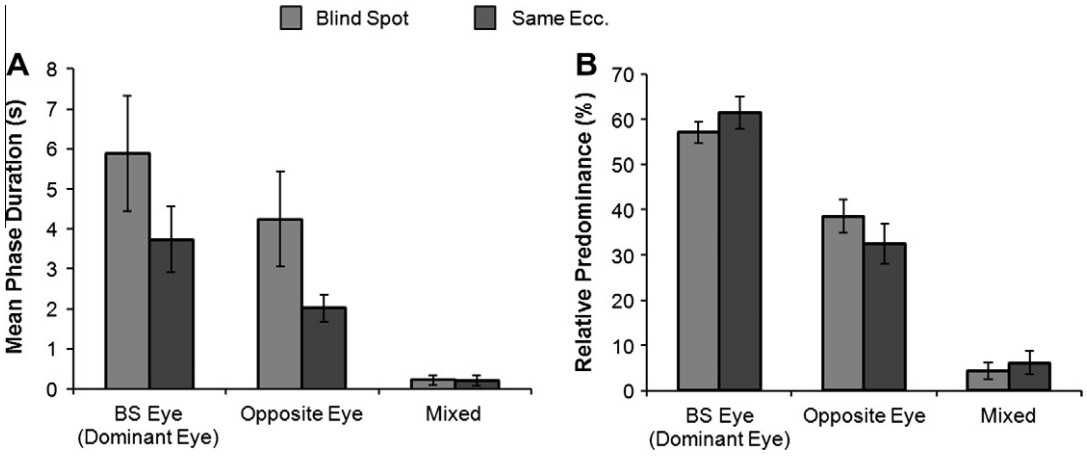

Fig. 4. (A) Average mean phase duration of each eye and a mixed percept depending on the condition. (B) Average relative predominance of the mean phase duration for each eye and a mixed percept. Even when the stimulus was located at the blind spot, the filled-in surface at the blind spot could compete with the real surface of the opposite eye. Error bars indicate the s.e.m.

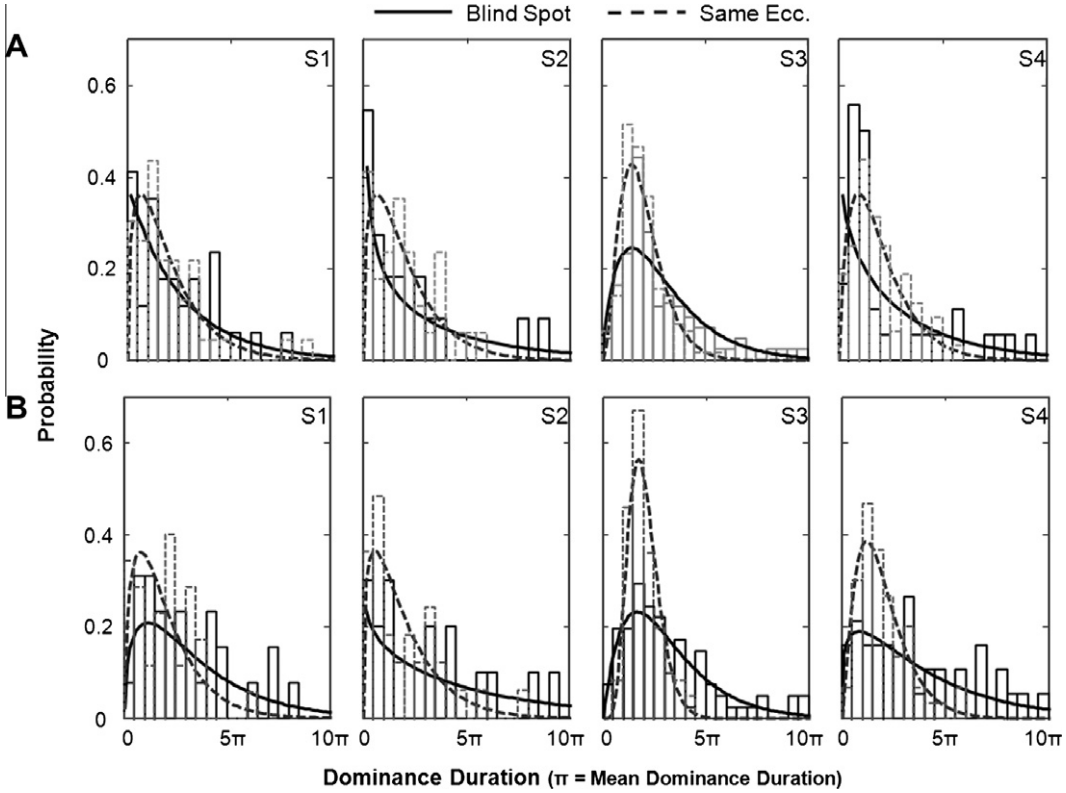

Fig. 5. Dominance duration distribution of each observer (S1–4) of the blind spot eye (A) and the opposite eye (B). The dominance durations were normalized by the individual baseline mean dominance duration (π), the mean dominance duration of the same eccentricity condition. The bars represent the probabilities of the dominance durations, and each of them was binned as 0.5π (solid bar: the blind spot condition; dashed bar: the same eccentricity condition). The curved lines indicate the fitted gamma functions of the blind spot (solid line) and the same eccentricity (dashed line) conditions.

duration of the ipsilateral eye (i.e., the dominance duration of the contralateral eye). Thus, the different mean dominance durations and relative predominance reported in Tong and Engel (2001) may originate from the increased dominance duration of the opposite eye rather than from the decreased dominance duration of the blind spot eye. This experiment showed that the filled-in surface at the blind spot also contributes to binocular rivalry and that the reduced strength of the filled-in surface is reflected in the modulated dominance duration distribution of the opposite eye.

4. Experiment 3: travelling waves through the blind spot

Travelling waves refer to the tendency for switches in rivalry state to arise within a local region of a rival target and, then, to spread in a wave-like fashion throughout the rest of that target. These state transitions can be exogenously triggered by abruptly increasing the contrast within one region of a suppressed stimulus, thereby producing a travelling wave whose origin is under stimulus control (Wilson, Blake, & Lee, 2001). In the present experiment, we tested whether waves could travel over the blind spot. It is known that waves can travel over a relatively small gap, but the effect of a trigger is weakened or abolished as the gap size increases (Kang, Heeger, & Blake, 2009; Kim, Blake, & Lee, 2005; Wilson et al., 2001). The size of the blind spot is much larger (6–8°; Armaly, 1969) than the size of the gap that blocks the spread of travelling waves reported in those earlier studies (0.3–1.0°; Kang, Heeger, & Blake, 2009; Wilson et al., 2001). Therefore, we felt it would be interesting to discover whether waves can travel over the blind spot with the aid of the filled-in surface. In addition, given that travelling waves involve the propagation of cortical activity (Lee, Blake, & Heeger, 2005, 2007), observing travelling waves at the blind spot would elucidate the neural basis of the filling-in of the blind spot.

Kang, Heeger, and Blake (2009) showed that travelling waves could be studied by periodically presenting triggers at opposite ends of two rival stimuli while observers simply track rivalry occurring within a restricted region of those stimuli; evidence for travelling waves is revealed by the entrainment of switches in dominance within the monitored region. This method requires observers to monitor only a small portion of the stimuli, a significant advantage when using eccentrically viewed rival stimuli as required in this experiment.

4.1. Materials and methods

4.1.1. Observers

Eight observers including the authors participated in this experiment. All reported normal or corrected-to-normal vision.

4.1.2. Apparatus

We used two CRT monitors (Samsung SyncMaster 2100MB; refresh rate, 85 Hz; resolution, 1600 × 1200) in this experiment. As a consequence of this change, the viewing distance was 60 cm and one pixel was subtended by approximately 0.020°. Also, the luminance of the background was 31.76 cd/m^2.

4.1.3. Stimuli

4.1.3.1. The fixation cross and gratings of rectangular shape. Examples of the stimuli are shown in Fig. 6. The fixation cross was the same as in previous experiments, but the locations of the fixation cross differed owing to the different design and monitors. The fixation cross was located 14.32° from the top and 7.16° from the left

or the right edge of the display depending on which eye's blind spot was tested in the blind spot condition. In the same eccentricity condition, the fixation cross was located 19.10° from the left or right edge and 3.58° from the top of the display to present the same stimuli of the blind spot condition to the same eccentricity, but not at the blind spot. The stimuli were presented vertically at the location corresponding to the blind spot in the blind spot condition or horizontally below the fixation with the same distance used with the blind spot in the same eccentricity condition.

Gratings within a rectangular aperture were again used as stimuli. The width of the grating was set for each observer to be 75% of the horizontal length of the blind spot. The length of the grating was individually determined by the minimal stimulus length measurement procedure. The same lengths and widths were used in the same eccentricity conditions. The spatial frequency of the gratings was 2.5 cycles per rectangle width, and the gratings were tilted 45° clockwise or counterclockwise. The Michelson contrast of the gratings was 74.29%.

4.1.3.2. Tracking region and a trigger. Because of the peripheral location of the blind spot, it would be difficult to track the entire path of the travelling waves, i.e., the technique used by Wilson et al. (2001) in their original study of travelling waves. Instead, we used stimuli, similar to those designed by Kang, Heeger, and Blake (2009), and only local percepts were monitored (tracking region, similar to Experiment 2). The tracking region was indicated by four dots, two at the left and the other two at the right sides of the grating, and the diameter of each dot was 0.5° (Fig. 6A). The two dots near the blind spot were presented 0.5° above or below the blind spot, and the other two dots were presented 2° above or below the dots near the blind spot. All configurations were rotated 90° in the same eccentricity conditions.

The trigger was separated by 1° from the blind spot and was always presented on the side opposite that of the tracking region. The width of the trigger was 1° and its contrast was abruptly increased to 99.05% for 50 ms. The trigger also changed its phase by 180° to make it more salient.

4.1.4. Design

There were four within-subject variables. First, the testing location was varied: it was either at the blind spot or the same eccentricity outside the blind spot. The second variable was whether or not there were triggers: the no-trigger condition served as the baseline to determine the time to trigger. These two variables were tested in separate blocks. The baseline blocks preceded the trigger blocks because we used the mean phase durations from the baseline block to determine the timing of the contrast increment in the trigger blocks. In addition, there was a condition in which the rival stimuli were located at the same place as that used in the same eccentricity condition, except now those rival targets contained actual gaps that matched the size of the blind spot (Fig. 6C); the gaps were produced by setting the contrast of the rival stimuli to zero within that gap region. Thus, there were 5 blocks in total. The other two variables were the locations of the tracking region (above or below the blind spot in the blind spot condition; peripheral or central in the same eccentricity conditions) and the orientation of the

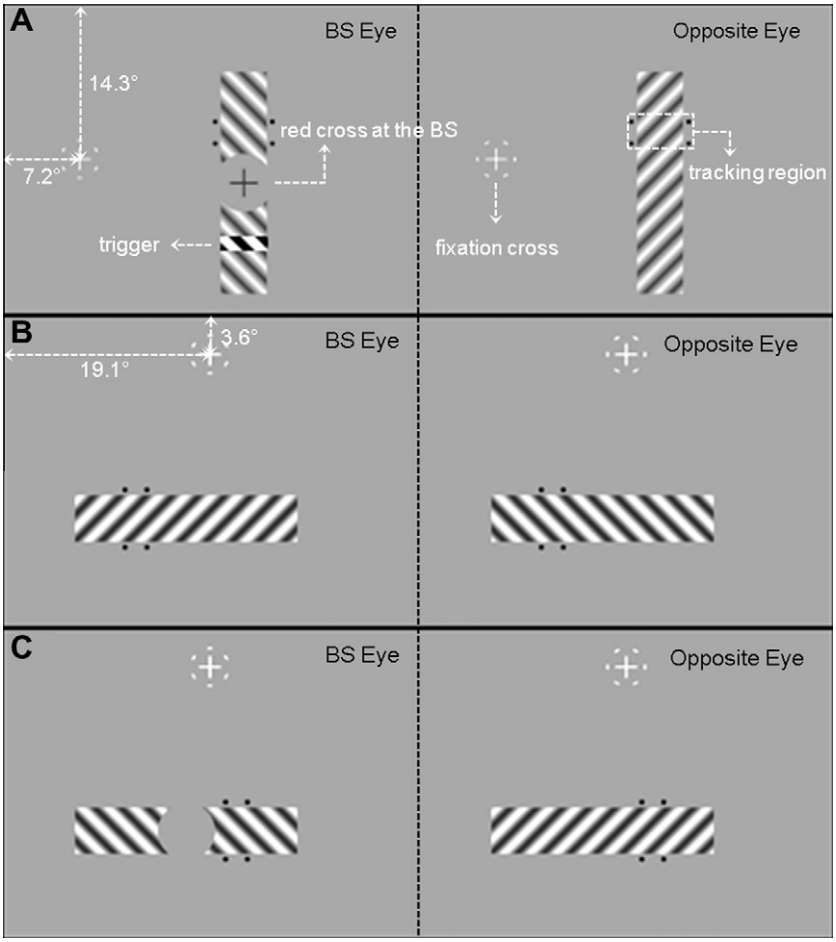

Fig. 6. Examples of stimuli in Experiment 3. (A) The blind spot condition with the trigger. (B) The same eccentricity condition. (C) The same eccentricity with a hole condition. Note that the hole in the middle of the grating is not the blind spot but a blind-spot-sized mask.

gratings (clockwise or counterclockwise). These two variables were tested in separate trials and were randomized in a block. Each trial lasted for 90 s. The trigger condition was repeated twice. Thus, there were 32 trials in total (Baseline blocks (2 testing locations × 2 tracking locations × 2 grating tilts) + Trigger blocks (3 testing locations × 2 tracking locations × 2 grating tilts × 2 iterations) = 32 trials). There was a 2-min rest period at the beginning of each block and between each trial.

4.1.5. Procedure

First, the location of the blind spot of each observer's dominant eye was measured using the same procedure as that used in Experiment 2. Next, the blind spot indicator was drawn as a circle instead of a polygon in this experiment to facilitate filling-in. The radius of the blind spot indicator was the shortest radius of the blind spot. The length of the stimuli was then individually determined to produce filling-in. Observers adjusted the length of the grating presented to the blind spot eye until filling-in was achieved. This procedure was repeated four times, twice for each grating tilt, and the average of these four measurements was used in the main experiment.

Each trial began with presentation of the fixation mark, the blind spot indicator, and the red cross; observers used this time to confirm their fixation. After the fixation check, the indicator disappeared, leaving only the fixation and red crosses. The orthogonally oriented, dichoptic rival gratings were then presented, one to the blind spot eye and the other to the opposite eye. In the triggering blocks, the high-contrast trigger was presented for 50 ms to the blind spot eye when the stimulus of the opposite eye was being perceived for more than one third of its mean phase duration, which was previously measured in the baseline blocks. The task was to report the perceived orientation of the test gratings within the tracking region. Observers pressed the '1' key for a counterclockwise grating and the '2' key for a clockwise grating for 90 s. Both keys were pressed simultaneously to signify mixed percepts.

4.2. Results and discussion

First, the analysis of the dominance durations revealed approximately equal periods of dominance for each eye's rival stimulus (mean dominance duration: 2929 ms; s.e.m.: 259 ms) and a low proportion of a mixed percept (mean: 264 ms; s.e.m.: 104 ms). There was no significant main effect of the test locations, eye, or the existence of a trigger on the mean dominance duration. Also, the relative predominance was fairly even (mean relative predominance of each eye: 46.26%; s.e.m.: 1.29%, mean relative predominance of a mixed percept: 3.74%, s.e.m.: 1.29%).

Before further analyses, the data were normalized by the individual baseline mean dominance durations of the opposite eye (π) of each testing location to compare the effects of triggering across conditions. The baseline mean dominance durations were derived from the mean phase durations in the baseline blocks. Then, we computed the event-related probabilities of the blind spot eye dominance across times relative to the value of π from the onset of the opposite eye dominance to 2π (Fig. 7). Because the triggers were given when the blind spot eye was suppressed for more than one third of π, the probability of a transition at the beginning of each event was always zero. In contrast to the experiment by Kang, Heeger, and Blake (2009), we did not trigger both stimuli in turn but only triggered the stimulus in the blind spot eye, as our purpose was to learn whether waves travelled over the blind spot. Thus, as time elapsed from the onset, the probability would rise to 0.5 at around π with some variance and would then fluctuate irregularly around the value of 0.5 as the effect of the trigger dissipated. If the trigger induced travelling waves of dominance, the probability of reporting the blind spot eye stimulus

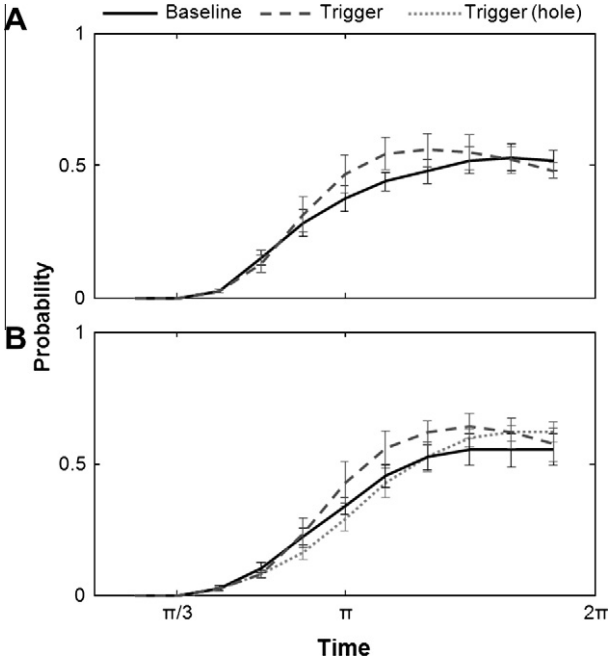

Fig. 7. Mean probability of eight observers reporting the blind spot eye stimulus at the blind spot (A) and at the same eccentricity outside the blind spot (B). The time was normalized by the individual baseline mean phase duration (π), the mean phase duration of the baseline conditions. The bin size was one sixth of the value of π. The starting point of the time indicates the onset of reporting that observers perceive the stimulus of the opposite eye. The onset of the trigger was one third of π. The error bars indicate the s.e.m.

would be highest at and around the π, and the slope of the function would be steeper than that of the baseline blocks. These trends are reflected in the maximum value of the probability and the latency of the maximum value.

The same eccentricity condition showed a clear effect of the trigger (Fig. 8, right, light gray). The result of paired-sample *t*-tests of the maximum value and its latency between the baseline block and the triggered block was significant (Maximum: $t(7) = 3.14$, $p < .05$; Latency: $t(7) = 2.38$, $p < .05$). This result indicates that rivalry alternations were being influenced by triggers presented within the region outside the blind spot, consistent with the results of Kang, Heeger, and Blake (2009). When there was a gap between the trigger and the tracking region, however, the effect of the trigger was not significant (Fig. 8 right, dark gray; Maximum: $t(7) = 1.25$, $p = .25$; Latency: $t(7) = .55$, $p = .60$), implying that travelling waves were not able to traverse a gap region the size of the blind spot. Remarkably, the blind spot itself did not impair the progress of travelling waves, as evidenced by the significant effect of the trigger in the blind spot condition (Fig. 8 left, light gray). The maximum value of the triggered block was significantly higher and its latency was shorter (Maximum: $t(7) = 2.74$, $p < .05$; Latency: $t(7) = 3.33$, $p < .05$) than the baseline.

We also estimated the speed of the travelling wave. It was 18.15 ± 7.12 deg/s in the blind spot and 30.26 ± 20.07 deg/s in the same eccentricity condition. It was 3.65 ± 0.54 deg/s when the eccentricity was 1.8° in Wilson et al. (2001). This speed was almost doubled when the eccentricity was doubled in their study. Therefore, the speed measured in our study was similar to that in their study because our eccentricity value was 15.79°. Although the estimated speed in the blind spot condition appeared to be slower than that of the same eccentricity condition, this difference was not statistically significant ($t(7) = .93$, $p = .38$) on account of large individual differences. This is also consistent with the finding that the maximum value of the probability and the latency of the

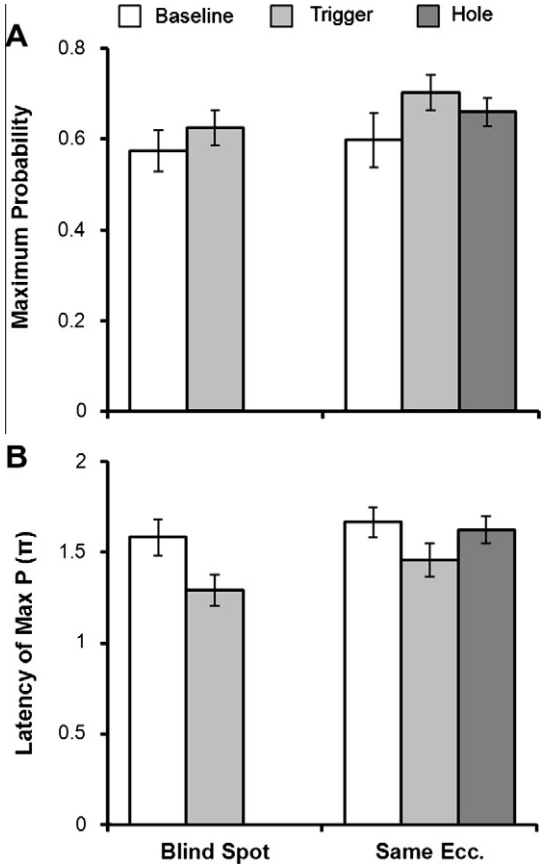

Fig. 8. Maximum probability of blind spot eye dominance (A) and its latency (B). The latency of the maximum probability was normalized by the baseline mean phase duration (π). The error bars indicate the s.e.m.

maximum value did not differ between the blind spot and same eccentricity conditions with the trigger (Maximum: $t(7) = 2.09$, $p = .08$; Latency: $t(7) = 1.53$, $p = .17$).

The results of this experiment imply that perceptual waves can indeed travel across the blind spot, and it is interesting to consider the implication of this finding in the context of the neural model of dominance wave propagation proposed by Wilson et al. (2001). According to that model, two groups of neurons selectively responsive to each rivaling stimulus exert reciprocal inhibition on one another via inhibitory interneurons. Perceptual dominance occurs when one group of neurons strongly inhibits the other group. Over time inhibition strength exerted by the dominant neural group decreases because of adaptation of those neurons, and eventually the other group will be released from inhibition and achieve temporary dominance. More importantly for interpretation of our results, when the inhibition of interneurons between rivaling stimuli spreads spatially as in our stimuli, this disinhibition will occur recurrently within the retinotopic representation of an extended rival target. This recurrent disinhibition generates a wave of state transitions and, thus, the impression of one percept sweeping the other out of awareness. Viewed within this framework, the ability of a triggered wave to traverse the blind spot implies that the filled-in surface within the blind spot carries neural signals underlying this wave-like spread of dominance.

5. General discussion

This study used surface filling and binocular rivalry to investigate the characteristics of perceptual filling-in of the blind spot. Results from Experiment 1 revealed that a pattern was able to fill the blind spot more readily when the pattern's contours were collinear as opposed to orthogonal ("more readily" meaning that the minimal length of the long axis of a pattern producing filling-in could be shorter for the collinear contours compared to orthogonal contours). Filling-in was also more effective when the patterns had smaller difference in orientation. Thus, the orientation properties of a pattern falling partly within the blind spot influence that pattern's ability to fill in the blind spot, in a manner reminiscent of contour integration (Field, Hayes, & Hess, 1993) and amodal completion (Kellman & Shipley, 1991).

Experiment 2 measured the dynamics of binocular rivalry when one portion of a rival pattern fell within the blind spot but nonetheless appeared continuous throughout the pattern. Compared to the condition where the pattern was genuinely continuous, the filled-in pattern altered the durations of suppression of that pattern, resulting in fewer short-duration states and more long-duration states. This pattern of results is consistent with Levelt's second proposition (Levelt, 1968), wherein variations in the stimulus strength of a rival pattern alter its durations of suppression (which is the same as saying those variations alter the durations of dominance of the stimulus in the contralateral eye). Now, one could argue that the findings of Experiments 2 do not arise because the filled-in surface is weaker relative to the real surface but because the sensitivity of the area in the opposite eye corresponding to the blind spot is higher than that of other regions at the same eccentricity (Wolf & Gardiner, 1963). In line with this, several studies reporting differences between the filled-in surface at the blind spot and the real surface also attributed those differences to the opposite eye's higher sensitivity in this region (Cumming & Friend, 1980; He & Davis, 2001; Maertens & Pollmann, 2007). However, this explanation seems less likely when considering Levelt's second proposition (Levelt, 1968). If the stimulus presented to the region corresponding to the other eye's blind spot is more strongly represented than the stimulus of the same eccentricity due to the higher sensitivity in this region, the distribution of dominance durations should change in the blind spot eye, not in the opposite eye as in Experiment 2. Thus based on Levelt's proposition, it appears that the higher sensitivity of the opposite eye in the corresponding region of the blind spot is not the main factor influencing the dynamics of rivalry.

The reduced strength of the blind spot representation as compared to the real surface observed in Experiment 2 is consistent with the results of an electrophysiological study of macaque visual cortex (Matsumoto & Komatsu, 2005). Even when a bar stimulus was long enough to yield blind spot filling, the responses of the neurons whose receptive fields overlapped the blind spot were not as potent as those of neurons activated by a stimulus imaged in the opposite eye at the retinal area corresponding to the other eye's blind spot.

Experiment 3 established that travelling waves of binocular rivalry dominance can propagate through the blind spot, carrying the wave of dominance from one end of a rival stimulus to the other. The same is not true, however, when a real gap (the size of the blind spot) is situated within a rival stimulus imaged outside of the blind spot. Evidently, then, the process responsible for filling-in at the blind spot can also promote neural events supporting travelling waves of dominance in rivalry.

Some previous studies of the blind spot have shown similarities between filled-in surfaces and real surfaces, using measures such as interocular transfer of motion aftereffects (Murakami, 1995) and dominance durations during binocular rivalry (He & Davis, 2001; Tong & Engel, 2001). However, other studies have found differences between them. For example, an adapting pattern falling partially within the blind spot does not produce a tilt aftereffect (Cumming & Friend, 1980) nor does it generate illusory contours

(Maertens & Pollmann, 2007). In the present study, we observed both similarities and differences between real and filled-in stimuli. Specifically, Experiment 1 found that contour collinearity had influence on filled-in stimuli, and Experiments 2 and 3 showed that a filled-in surface can impact binocular rivalry and the spatio-temporal spread of rivalry dominance. At the same time, Experiment 2 revealed that a filled-in pattern exhibited diminished strength in terms of its emergence from interocular suppression. Why do those similarities and differences occur, and can they be understood within a unified theoretical framework? To answer those questions, we turn to neural models of blind spot filling-in.

Komatsu, Kinoshita, and Murakami (2000) proposed that when the blind spot falls within the interior of an image of a large uniform surface, neurons in layer 6 of V1 with very large receptive fields are activated, creating activity that mimics a complete, filled-in surface. According to their model, there are three possible sources of information to the blind spot representation in V1: afferents from the lateral geniculate nucleus (LGN), horizontal connection within V1, and feedback from extrastriate cortex. Among those three, the results of Experiment 1 suggest that contour information within an area surrounding the blind spot is integrated by way of long-range horizontal connections of the sort known to exist within V1 (Crook, Engelmann, & Löwel, 2002; Gilbert & Wiesel, 1989).

For purposes of accounting for the results of Experiments 2 and 3, however, this model is incomplete for it ignores differential influences from retinal areas in the eye opposite that of the blind spot. This limitation in the model could be rectified by the addition of long-range dichoptic horizontal cortical connections between neurons near the blind spot and neurons in the opposite eye whose receptive fields correspond to the blind spot region; indeed, just such an idea has been proposed by Tripathy and Levi (1994). With this change, the neural model of filling-in could account for the results of Experiments 2 and 3. This binocular interaction is also used for explaining the mechanism of binocular rivalry (Freeman, 2005; Lumer, 1998; Stollenwerk & Bode, 2003) and travelling waves (Kang et al., 2011; Knapen, van Ee, & Blake, 2007; Wilson et al., 2001), which we used in Experiments 2 and 3, respectively.

5.1. Conclusion

In summary, the current study investigated the properties of filling-in at the blind spot by comparing these properties to those associated with a real surface. The results suggest a common mechanism as normal perception is shared, with the filled-in surface playing a role in binocular rivalry but at a reduced strength. Including the present study into the blind spot model will specify the blind spot filling-in mechanism, especially in terms of binocular interactions.

Acknowledgments

This work was supported by a grant from the National Research Foundation of Korea (NRF) funded by the Korean Government (MEST, No. 2010-0029270). For helpful comments and discussion on this manuscript, we thank Dr. Randolph Blake.

References

Aafjes, M., Hueting, J. E., & Visser, P. (1966). Individual and interindividual differences in binocular retinal rivalry in man. *Psychophysiology, 3*(1), 18–22.

Abadi, R. V., Jeffery, G., & Murphy, J. S. (2011). Awareness and filling-in of the human blind spot: Linking psychophysics with retinal topography. *Investigative Ophthalmology & Visual Science, 52*(1), 541–548.

Alais, D., & Blake, R. (1999). Grouping visual features during binocular rivalry. *Vision Research, 39*(26), 4341–4353.

Araragi, Y., & Nakamizo, S. (2008). Anisotropy of tolerance of perceptual completion at the blind spot. *Vision Research, 48*(4), 618–625.

Armaly, M. F. (1969). The size and location of the normal blind spot. *Archives of Ophthalmology, 81*(2), 192–201.

Awater, H., Kerlin, J. R., Evans, K. K., & Tong, F. (2005). Cortical representation of space around the blind spot. *Journal of Neurophysiology, 94*(5), 3314–3324.

Blake, R. R., Fox, R., & McIntyre, C. (1971). Stochastic properties of stabilized-image binocular rivalry alternations. *Journal of Experimental Psychology, 88*(3), 327–332.

Brainard, D. H. (1997). The psychophysics toolbox. *Spatial Vision, 10*(4), 433–436.

Brascamp, J. W., van Ee, R., Pestman, W. R., & van den Berg, A. V. (2005). Distributions of alternation rates in various forms of bistable perception. *Journal of Vision, 5*(4), 287–298.

Collins, J. F., & Blackwell, L. K. (1974). Effects of eye dominance and retinal distance on binocular rivalry. *Perceptual and Motor Skills, 39*(2), 747–754.

Crook, J. M., Engelmann, R., & Löwel, S. (2002). GABA-inactivation attenuates colinear facilitation in cat primary visual cortex. *Experimental Brain Research, 143*(3), 295–302.

Cumming, G., & Friend, H. (1980). Perception at the blind spot and tilt aftereffect. *Perception, 9*(2), 233–238.

Dennett, D. C. (1992). Filling in versus finding out: A ubiquitous confusion in cognitive science. In: Pick, Van den Broek, Knill (Eds.), *Cognition, conception, and methodological issues*. American Psychological Association.

Field, D. J., Hayes, A., & Hess, R. F. (1993). Contour integration by the human visual system: Evidence for a local "association field". *Vision Research, 33*(2), 173–193.

Fox, R., & Herrmann, J. (1967). Stochastic properties of binocular rivalry alternations. *Perception and Psychophysics, 2*, 432–436.

Freeman, A. W. (2005). Multistage model for binocular rivalry. *Journal of Neurophysiology, 94*(6), 4412–4420.

Geisler, W. S., Perry, J. S., Super, B. J., & Gallogly, D. P. (2001). Edge co-occurrence in natural images predicts contour grouping performance. *Vision Research, 41*(6), 711–724.

Gilbert, C. D., & Wiesel, T. N. (1989). Columnar specificity of intrinsic horizontal and corticocortical connections in cat visual cortex. *The Journal of Neuroscience, 9*(7), 2432.

Grossberg, S., & Mingolla, E. (1985). Neural dynamics of perceptual grouping: Textures, boundaries, and emergent segmentations. *Percept and Psychophysics, 38*(2), 141–171.

He, S., & Davis, W. L. (2001). Filling-in at the natural blind spot contributes to binocular rivalry. *Vision Research, 41*(7), 835–840.

Kang, M. S., Heeger, D., & Blake, R. (2009). Periodic perturbations producing phase-locked fluctuations in visual perception. *Journal of Vision, 9*(2), 1–12.

Kang, M. S., Lee, S. H., Kim, J., Heeger, D., & Blake, R. (2011). Modulation of spatiotemporal dynamics of binocular rivalry by collinear facilitation and pattern-dependent adaptation. *Journal of Vision, 10*(11), 1–15.

Kawabata, N. (1982). Visual information processing at the blind spot. *Perceptual and Motor Skills, 55*(1), 95–104.

Kawabata, N. (1983). Global interactions in perceptual completion at the blind spot. *Vision Research, 23*(3), 275–279.

Kellman, P. J., & Shipley, T. F. (1991). A theory of visual interpolation in object perception. *Cognitive Psychology, 23*(2), 141–221.

Kim, S. -I., Blake, R., & Lee, S. -H. (2005). When a traveling wave meets a gap on its way. *Journal of Vision, 5*(8), 2, 2a (Abstract). doi:10.1167/5.8.2. <http://journalofvision.org/5/8/2/>.

Knapen, T., van Ee, R., & Blake, R. (2007). Stimulus motion propels traveling waves in binocular rivalry. *PLoS One, 2*(1), e739.

Komatsu, H. (2006). The neural mechanisms of perceptual filling-in. *Nature Review Neuroscience, 7*(3), 220–231.

Komatsu, H., Kinoshita, M., & Murakami, I. (2000). Neural responses in the retinotopic representation of the blind spot in the macaque V1 to stimuli for perceptual filling-in. *Journal of Neuroscience, 20*(24), 9310–9319.

Komatsu, H., Kinoshita, M., & Murakami, I. (2002). Neural responses in the primary visual cortex of the monkey during perceptual filling-in at the blind spot. *Neuroscience Research, 44*(3), 231–236.

Lee, S. H., Blake, R., & Heeger, D. J. (2005). Traveling waves of activity in primary visual cortex during binocular rivalry. *Nature Neuroscience, 8*(1), 22–23.

Lee, S. H., Blake, R., & Heeger, D. J. (2007). Hierarchy of cortical responses underlying binocular rivalry. *Nature Neuroscience, 10*(8), 1048–1054.

Levelt, W. J. M. (1967). Note on the distribution of dominance times in binocular rivalry. *British Journal of Psychology, 58*(1), 143–145.

Levelt, W. J. M. (1968). *On binocular rivalry*. The Hague, the Netherlands: Mouton.

Lleras, A., & Moore, C. M. (2006). What you see is what you get: Functional equivalence of a perceptually filled-in surface and a physically presented stimulus. *Psychological Science, 17*(10), 876–881.

Logothetis, N. K. (1998). Single units and conscious vision. *Philosophical Transactions of the Royal Society B: Biological Sciences, 353*(1377), 1801–1818.

Lumer, E. D. (1998). A neural model of binocular integration and rivalry based on the coordination of action-potential timing in primary visual cortex. *Cerebral Cortex, 8*(6), 553–561.

Maertens, M., & Pollmann, S. (2007). Illusory contours do not pass through the "blind spot". *Journal of Cognitive Neuroscience, 19*(1), 91–101.

Matsumoto, M., & Komatsu, H. (2005). Neural responses in the macaque V1 to bar stimuli with various lengths presented on the blind spot. *Journal of Neurophysiology, 93*(5), 2374–2387.

Mueller, T. J., & Blake, R. (1989). A fresh look at the temporal dynamics of binocular rivalry. *Biological Cybernetics, 61*, 223–232.

Murakami, I. (1995). Motion aftereffect after monocular adaptation to filled-in motion at the blind spot. *Vision Research, 35*(8), 1041–1045.

Pelli, D. G. (1997). The VideoToolbox software for visual psychophysics: Transforming numbers into movies. *Spatial Vision, 10*(4), 437–442.
Pessoa, L., Thompson, E., & Noë, A. (1998). Finding out about filling-in: A guide to perceptual completion for visual science and the philosophy of perception. *Behavioral and Brain Science, 21*(6), 723–748 (discussion 748-802).
Ramachandran, V. S. (1992). Blind spots. *Scientific American, 266*(5), 86–91.
Shimojo, S., Kamitani, Y., & Nishida, S. (2001). Afterimage of perceptually filled-in surface. *Science, 293*(5535), 1677–1680.
Shin, I. J., Jung, D., & Chong, S. C. (2007). Interocular filling-in of the blind spot. *The Korean Journal of Experimental Psychology, 19*(3), 221–231.
Spillmann, L., Otte, T., Hamburger, K., & Magnussen, S. (2006). Perceptual filling-in from the edge of the blind spot. *Vision Research, 46*(25), 4252–4257.
Stollenwerk, L., & Bode, M. (2003). Lateral neural model of binocular rivalry. *Neural Computation, 15*(12), 2863–2882.
Tong, F., & Engel, S. A. (2001). Interocular rivalry revealed in the human cortical blind-spot representation. *Nature, 411*(6834), 195–199.
Tripathy, S. P., & Levi, D. M. (1994). Long-range dichoptic interactions in the human visual cortex in the region corresponding to the blind spot. *Vision Research, 34*(9), 1127–1138.
Tripathy, S. P., Levi, D. M., Ogmen, H., & Harden, C. (1995). Perceived length across the physiological blind spot. *Visual Neuroscience, 12*(2), 385–402.
Wilson, H. R., Blake, R., & Lee, S. H. (2001). Dynamics of travelling waves in visual perception. *Nature, 412*(6850), 907–910.
Wolf, E., & Gardiner, J. S. (1963). Sensitivity of the retinal area in one eye corresponding to the blind spot in the other eye. *Journal of the Optical Society of America, 53*(12), 1437–1440.